PPA/AL/8

Thermal Neutron Spectrum Distribution in TRIGA Fuels

UNIT TENAGA NUKLEAR, JABATAN PERDANA MENTERI
NUCLEAR ENERGY UNIT, PRIME MINISTER'S DEPARTMENT
MALAYSIA

PPA/AL/9

|35|

Thermal Neutron Spectrum Distribution In TRIGA Fuels

Gui Ah Auu
Unit Tenaga Nuklear
Kompleks PUSPATI
43000 Kajang
Malaysia

Susumu Harasawa
Institute For Atomic Energy
Rikkyo University
Nagasaka 2-5-1
Yokosuka 240-01
Japan

Shigehiro An
Faculty Of Engineering
Tokai University
1-8-12 Higasi-cho
Hoya-Shi 202
Japan

Second Asian Seminar On Research Reactors (ASRR-II)

22-26 May 1989
Jakarta, Indonesia

Thermal Neutron Spectrum Distribution In TRIGA Fuels

Abstract

The dependence of thermal neutron spectrum in TRIGA fuel cell on fuel temperature and TRIGA fuel types were studied using LIBP and THERMOS codes. Some characteristics of the TRIGA fuel including its prompt negative temperature coefficient of reactivity were explained using the results of the study.

Introduction

The TRIGA fuel consists of a homogeneous mixture of uranium and zirconium hydride with the atomic ratio of zirconium to hydrogen of about 1:1.6. The hydrogen atom in the zirconium hydride is the primary neutron moderator and it is quite strongly bound in the zirconium hydride lattice. The movement of the hydrogen atoms in the lattice can be described by a combination of the standard Einstein(optical) mode and the Debye(acoustic) mode. However, the acoustic mode is insignificant except at 0.02 eV or lower. The binding of the hydrogen atoms has given rise to some unique moderating properties of the TRIGA fuels. As TRIGA reactor is basically a thermal reactor, the distribution of thermal neutron spectrum in TRIGA fuels can provide a better understanding of the physics of the reactor.

The thermal neutron spectrum distribution in the TRIGA fuel was calculated using the LIBP and THERMOS codes. The LIBP code was used to prepare the scattering kernel library for THERMOS. The scattering kernels for hydrogen in zirconium hydride and water calculated by Ise et al.[1] using the UNCLE and GASKET-FLANGE code respectively,were input into LIBP in this study. The Haywood Otake[2] model was used to calculate the scattering kernels of hydrogen in water. The nuclear library prepared by LIBP was then used by THERMOS to calculate thermal neutron spectrum in the TRIGA fuel cell. THERMOS code used 30 groups for thermal neutrons having energies between 0.6E-4 eV to 1.125 eV as depicted in Table 1. The thermal neutron spectrum in the fuel cell as a function of the fuel meat temperature and the uranium content were investigated.

TRIGA Fuel Cell

The physical dimension of the Rikkyo University TRIGA Mark II fuel cell is used to represent the TRIGA fuel cell. The Rikkyo reactor uses aluminium cladded fuel rod with a fuel section of 35.56 cm(14 in). Although the Rikkyo reactor uses only the 8.5 w/o(uranium weight percent) fuel,the 12 w/o and 20 w/o fuels are also included in the study. Description of the TRIGA fuel cell and central thimble cell are summarized in Table 2 and 3 respectively.

Results And Discussions

The 30 thermal neutron groups are collapsed into the following four broad groups:

Group 1: 0.6E-4 eV to 0.046 eV
Group 2: 0.046 eV to 0.132 eV
Group 3: 0.123 eV to 0.425 eV
Group 4: 0.425 eV to 1.125 eV

Table 4 summarizes the neutron absorption rate in the 8.5 w/o fuel cell at 23 ^{o}C, 100 ^{o}C, 200 ^{o}C, 400 ^{o}C and 700 ^{o}C while Table 5 contains the ratio of the average thermal neutron flux in various regions of the fuel cell to that in the fuel cell., The distribution of thermal neutrons in the fuel cell at various fuel

Table 1. Thermal Neutron Energy Structure In THERMOS

	Upper·boundary		Mid point		Mesh width
	Energy (eV)	Velocity	Energy (eV)	Velocity	Velocity
1	0.00057	0.15	0.00023	0.1	0.1
2	0.00158	0.25	0.00101	0.2	0.1
3	0.00310	0.35	0.00228	0.3	0.1
4	0.00512	0.45	0.00405	0.4	0.1
5	0.00765	0.55	0.00632	0.5	0.1
6	0.01069	0.65	0.00911	0.6	0.1
7	0.01423	0.75	0.01240	0.7	0.1
8	0.01828	0.85	0.01619	0.8	0.1
9	0.02283	0.95	0.02049	0.9	0.1
10	0.02789	1.05	0.02530	1.0	0.1
11	0.03346	1.15	0.03061	1.1	0.1
12	0.03953	1.25	0.03643	1.2	0.1
13	0.04611	1.35	0.04276	1.3	0.1
14	0.05319	1.45	0.04959	1.4	0.1
15	0.06078	1.55	0.05692	1.5	0.1
16	0.07384	1.7084	0.06699	1.6273	0.15835
17	0.08970	1.8829	0.08138	1.7935	0.17453
18	0.10896	2.0752	0.09886	1.9767	0.19236
19	0.13236	2.2873	0.12009	2.1787	0.21201
20	0.16078	2.5209	0.14588	2.4013	0.23367
21	0.19531	2.7785	0.17721	2.6466	0.25754
22	0.23726	3.0623	0.21527	2.9169	0.28386
23	0.28821	3.3752	0.26150	3.2150	0.31285
24	0.35011	3.7200	0.31776	3.5434	0.34482
25	0.42530	4.1000	0.38588	3.9054	0.38004
26	0.51664	4.5189	0.46875	4.3044	0.41887
27	0.62759	4.9806	0.56942	4.7441	0.4616[illegible]
28	0.76238	5.4894	0.69171	5.2288	0.50883
29	0.92611	6.0502	0.84026	5.7630	0.56081
30	1.12500	6.6683	1.02070	6.3517	0.61810

Table 2. TRIGA Fuel Cell Description (*)

Region	Radius (cm)	Volume fraction	Nuclide	Atomic density (1E24 atoms/cc)		
				8.5 w/o	12 w/o	20 w/o
Fuel meat	1.7985	0.6112	U-235	2.5665E-4	3.3694E-4	5.9588E-4
			U-238	1.0258E-3	1.3234E-3	2.3798E-3
			Zr	3.7171E-2	3.1140E-2	3.0443E-2
			H(ZrH)	5.9474E-2	4.9824E-2	4.8709E-2
Clad	1.8745	0.0544	Al	6.0200E-2	6.0200E-2	6.0200E-2
Water	2.3062	0.3360	H	6.7000E-2	6.7000E-2	6.7000E-2
			O	3.3500E-2	3.3500E-2	3.3500E-2

Table 3. Central Thimble Cell Description

Region	Radius (cm)	Volume fraction	Nuclide	Atomic density (1E24 atoms/cc)
Water	1.695	0.5402	H	6.7000E-2
			O	3.3500E-2
Clad	1.905	0.1421	Al	6.0200E-2
Water	2.3062	0.3177	H	6.7000E-2
			O	3.3500E-2

(*) The dimensions of Rikkyo fuel cell was used. At present, the Rikkyo reactor uses only 8.5 w/o fuel elements.

Table 4. Relative Absorption Rate of Thermal Neutrons in the Fuel Cell (*)

Fuel meat temperature	Neutron group	Fuel meat	Clad	Water
23°C	1	0.4632	0.0040	0.0464
	2	0.3715	0.0026	0.0263
	3	0.0635	0.0004	0.0044
	4	0.0160	0.0001	0.0015
	Sum	0.9142	0.0071	0.0786
100°C	1	0.4428	0.0040	0.0469
	2	0.3740	0.0026	0.0271
	3	0.0645	0.0129	0.0054
	4	0.0179	0.0002	0.0016
	Sum	0.8992	0.0197	0.0810
200°C	1	0.3993	0.0037	0.0445
	2	0.3887	0.0028	0.0297
	3	0.1056	0.0007	0.0061
	4	0.0174	0.0001	0.0014
	Sum	0.9110	0.0073	0.0817
400°C	1	0.3280	0.0036	0.0458
	2	0.3851	0.0030	0.0321
	3	0.1732	0.0010	0.0083
	4	0.0184	0.0002	0.0015
	Sum	0.9047	0.0078	0.0877
700°C	1	0.2461	0.0035	0.0475
	2	0.3586	0.0031	0.0349
	3	0.2653	0.0015	0.0119
	4	0.0257	0.0002	0.0017
	Sum	0.8957	0.0083	0.0960

(*) The total absorption rate in the fuel cell is normalized to unity.

Table 5. Ratio of Region Average Thermal Neutron Flux to The Cell Average Thermal Flux

Region	Fuel meat temperature °C	Average flux ratio for neutron groups			
		1	2	3	4
Fuel meat	23	0.8221	0.9777	0.9805	0.9679
	100	0.8020	0.9705	1.016	0.9899
	200	0.7794	0.9522	1.056	1.018
	400	0.6957	0.9271	1.117	1.032
	700	0.5781	0.8647	1.140	1.092
Aluminium cladding	23	1.102	0.9899	0.9970	1.006
	100	1.117	0.9938	0.9676	0.9941
	200	1.128	1.0111	0.9476	0.9669
	400	1.181	1.038	0.9009	0.9531
	700	1.248	1.085	0.9030	0.9107
Water	23	1.303	1.042	1.036	1.056
	100	1.337	1.054	0.9774	1.019
	200	1.376	1.084	0.9177	0.9723
	400	1.517	1.134	0.8059	0.9506
	700	1.718	1.239	0.7646	0.8497

temperature are shown in Figure 1. The neutron flux values shown are relative values.

The graphs in Figure 1 clearly show that in the fuel meat region, the lower energy neutrons, especially the group 1 neutron, are greatly depressed as the fuel temperature increases. On the other hand, the population of higher energy neutrons, especially the group 3 neutrons increases significantly. The reverse occurs in the water region of the fuel cell but the changes are not as much. The slight depression of the thermal neutrons flux at the fuel clad(inner radius 1.80 cm) is due to the absorption of thermal neutrons by the aluminium clad. These observations can be explained as follows:

When the fuel temperature increases, the temperature of the hydrogen moderator increases simultaneously because it is homogeneously mixed with the fuel. This reduces the moderating capacity of the hydrogen atoms and as a result of this, the fraction of higher energy neutrons in the fuel meat region increases accompanied by a decrease in the group 1 neutron population. According to the Einstein model mentioned earlier, the hydrogen atoms in the zirconium hydride lattice cannot slow down neutrons with energy lower than 0.14 eV but can instead upscatter these neutrons to a higher enegry level by imparting a multiple of 0.14 eV to them. Thus the population of the higher energy neutrons, especially the group 3 neutron which includes the 0.14 eV neutrons increases. The changes of the thermal neutron spectrum in the water region is less because the water temperature does not change as much as the fuel meat temperature since the heat generated in the fuel meat will take some time to be transferred to water through the clad. In addition, the hydrogen atoms in water are not so strongly bound as those in the fuel, and are able to

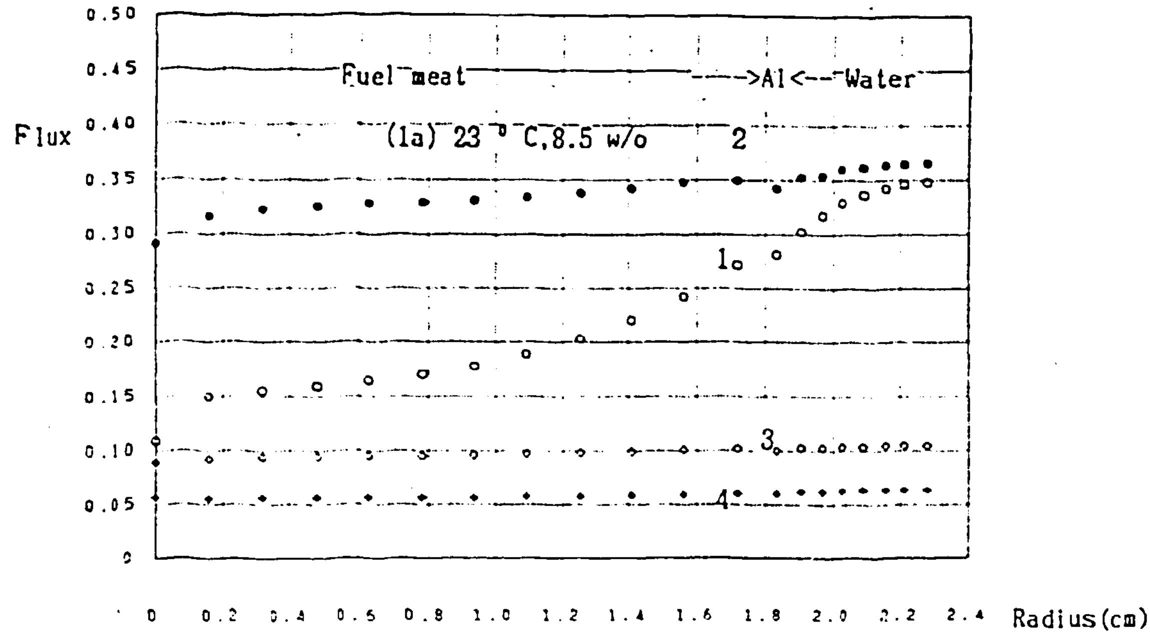
Flux
Fuel meat
>Al<--Water
(1a) 23 °C, 8.5 w/o
Radius(cm)

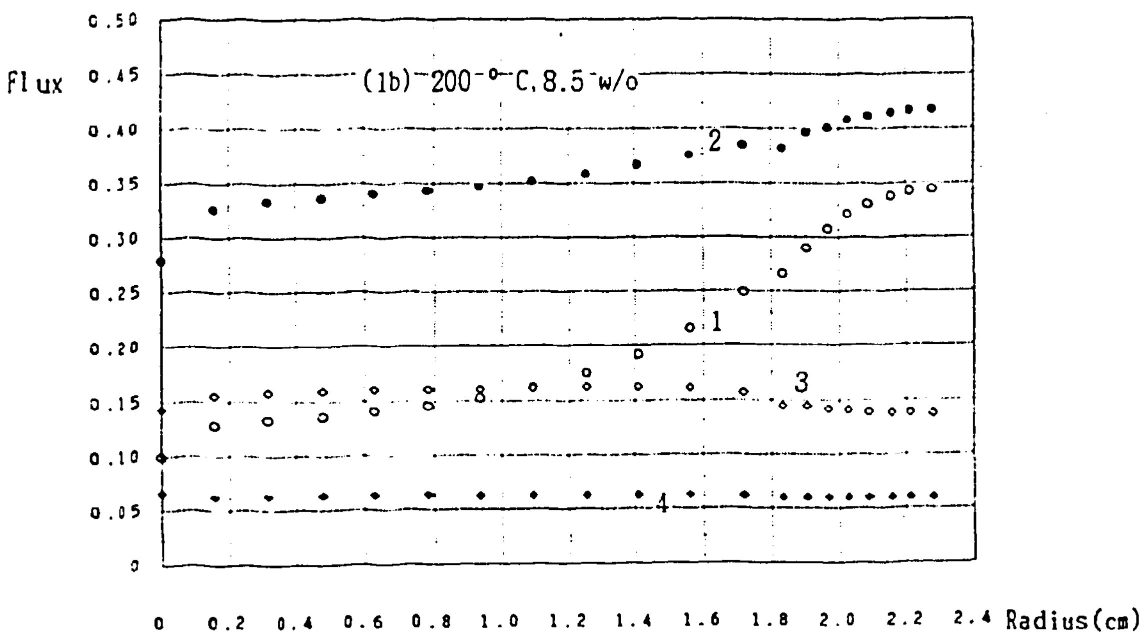
Flux
(1b) 200 °C, 8.5 w/o
Radius(cm)

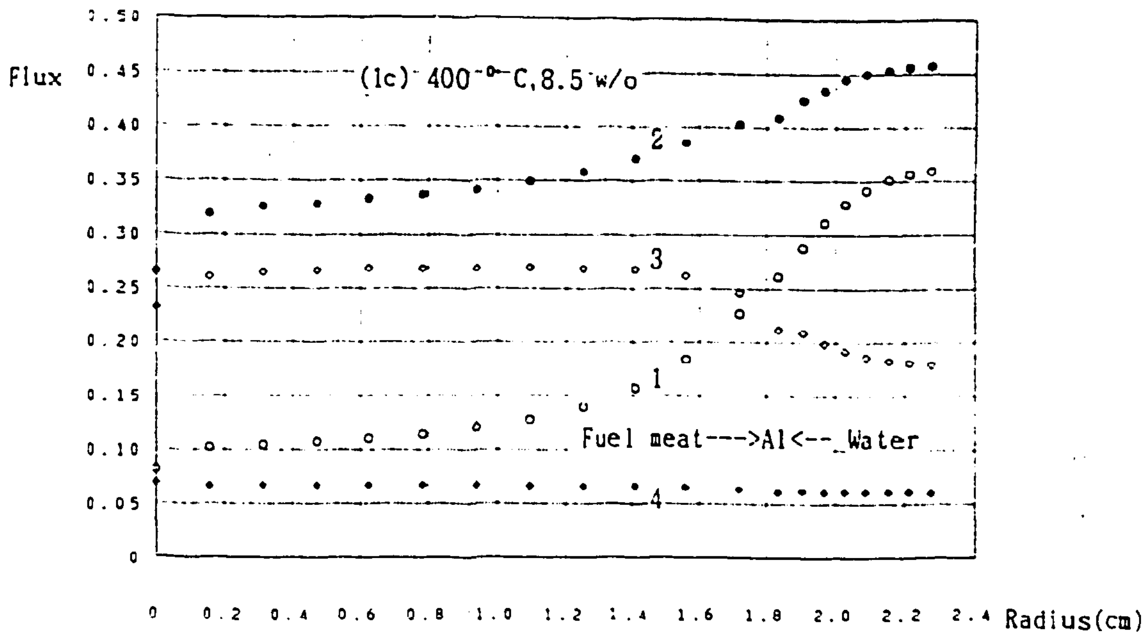

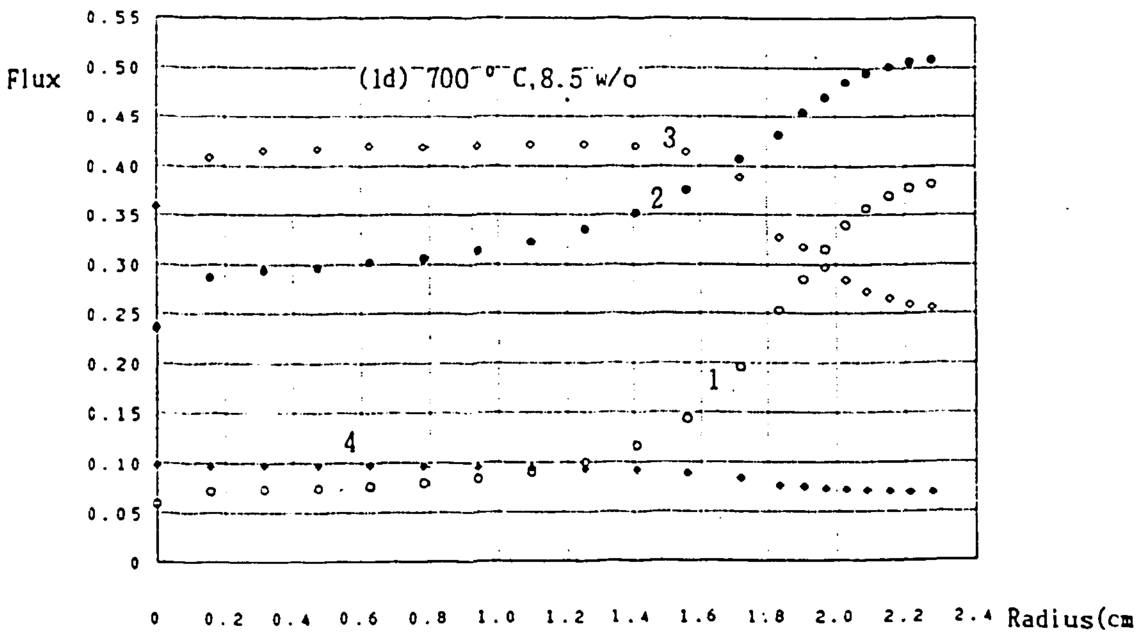

Figure 1. Thermal neutron spectrum distribution in 8.5 w/o fuel cell at various fuel meat temperatures.The numbers on the graphs correspond to the neutron groups.

slow down neutrons with energy lower than 0.14 eV.

As the average energy of the neutrons in the fuel meat increases, the probability for them to leak out of the fuel increases. The neutrons escaping from the fuel are quickly slowed down when they enter the water region and many of them are subsequently absorbed. Thus as the fuel temperature increases, the fraction of thermal neutron absorbed in the fuel meat decreases. However, the reverse occurs in the water region as shown in Tables 4 and 5.

The thermal neutron distribution in the 12 w/o and 20 w/o TRIGA fuel cells at several fuel meat temperatures are shown in Figure 2. The general trend of variation of the thermal neutron spectrum with fuel temperature for these fuels is similar to that of the 8.5 w/o fuel. However, as the uranium content of the fuel increases, the fraction of group 1 neutron population become more depressed. It should be noted that as the weight fraction of uranium in the fuel increases, the weight fraction of zirconium hydride decreases. This results in more thermal neutron absorption in the fuel due to higher uranium concentration but less neutron thermalization because of lower hydrogen concentration.

The thermal neutron distributions for the central thimble cell at $23^{o}C$ and $50^{o}C$ are displayed in Figure 3. The temperatures of the water and aluminium tube in the cell are assumed to be the same. Since the absorption cross-section of water is much less than that of uranium and water can slow down neutrons to 0.025 eV, the fraction of the group 1 neutron in the central thimble cell is much higher than that in the fuel cell. As the temperature of the water increases, the fraction of group 2 neutron increases much more than those in the other groups. This difference in the thermal neu-

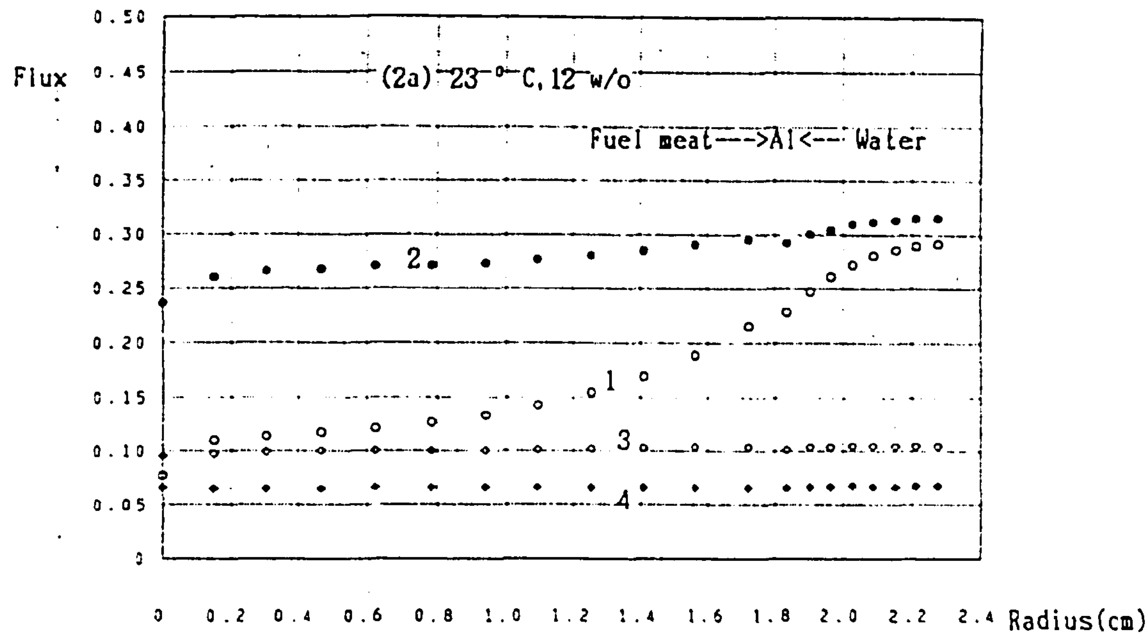
Flux
0.50
0.45
0.40
0.35
0.30
0.25
0.20
0.15
0.10
0.05
0
(2a) 23 °C, 12 w/o
Fuel meat--->Al<--- Water
2
1
3
4
0 0.2 0.4 0.6 0.8 1.0 1.2 1.4 1.6 1.8 2.0 2.2 2.4 Radius(cm)

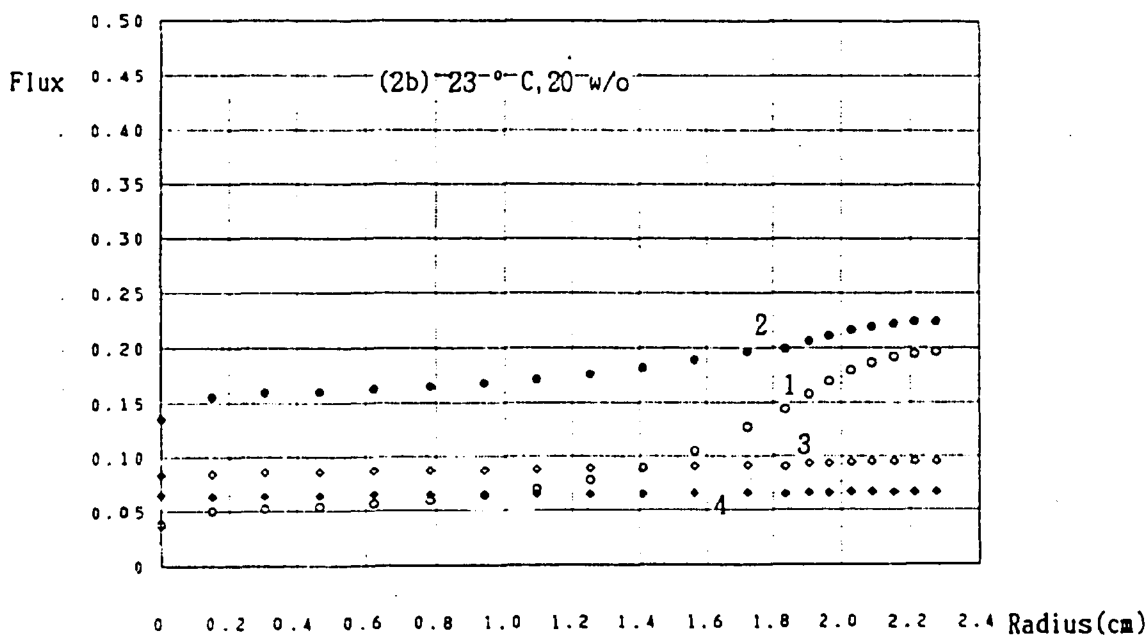
Flux
0.50
0.45
0.40
0.35
0.30
0.25
0.20
0.15
0.10
0.05
0
(2b) 23 °C, 20 w/o
2
1
3
4
0 0.2 0.4 0.6 0.8 1.0 1.2 1.4 1.6 1.8 2.0 2.2 2.4 Radius(cm)

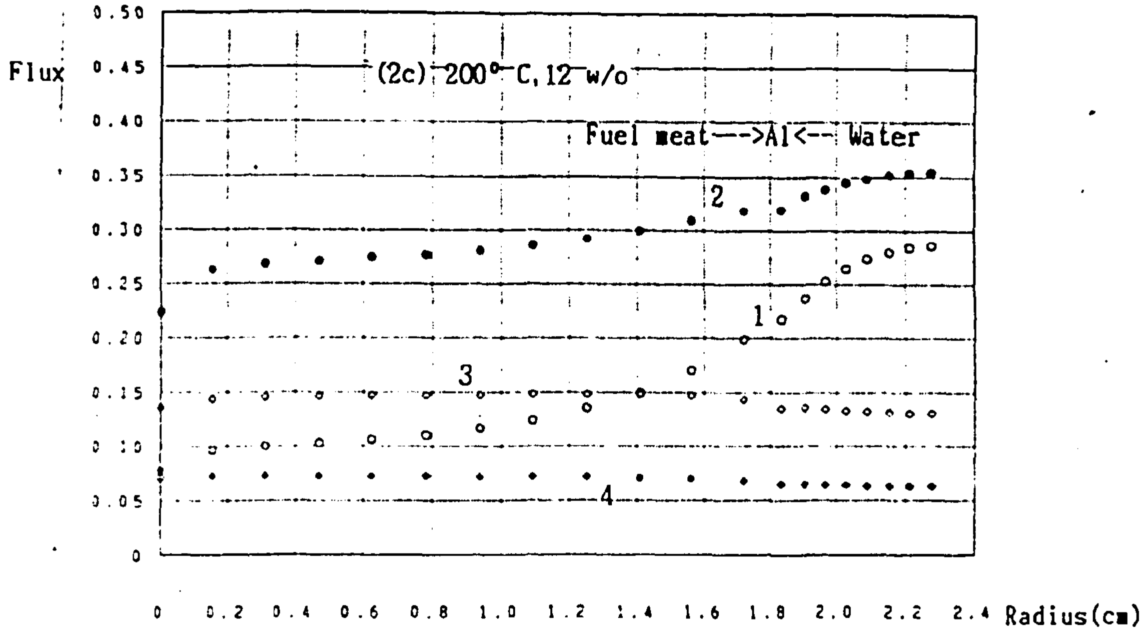
Flux
0.50
0.45
0.40
0.35
0.30
0.25
0.20
0.15
0.10
0.05
0
(2c) 200° C, 12 w/o
Fuel meat—>Al<-- Water
1
2
3
4
0 0.2 0.4 0.6 0.8 1.0 1.2 1.4 1.6 1.8 2.0 2.2 2.4 Radius(cm)

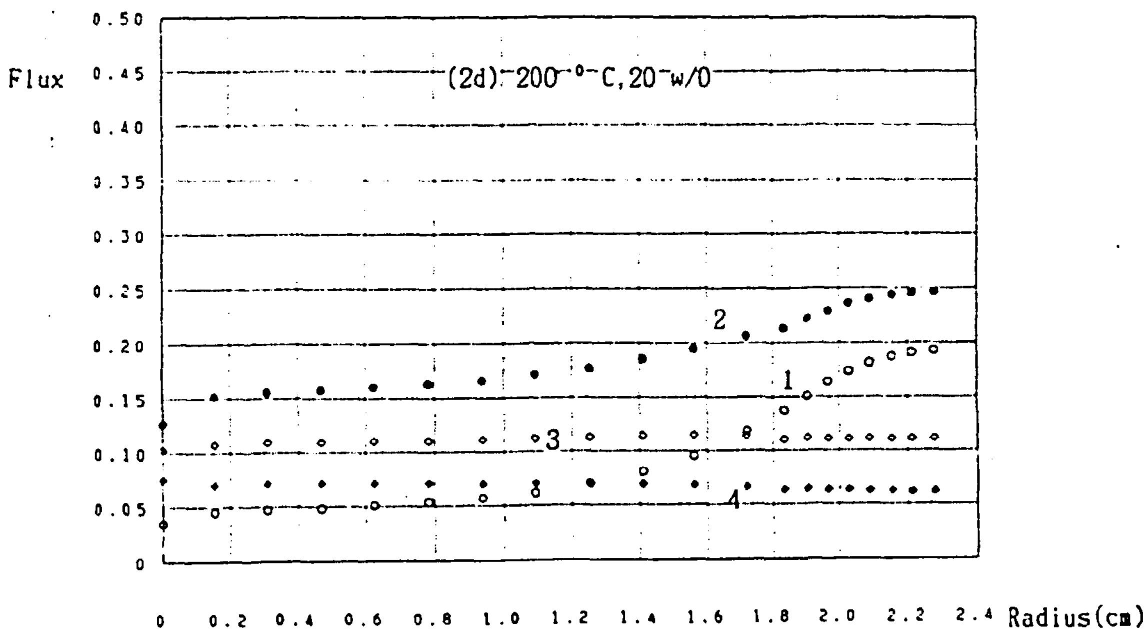
Flux
0.50
0.45
0.40
0.35
0.30
0.25
0.20
0.15
0.10
0.05
0
(2d) 200° C, 20 w/0
1
2
3
4
0 0.2 0.4 0.6 0.8 1.0 1.2 1.4 1.6 1.8 2.0 2.2 2.4 Radius(cm)

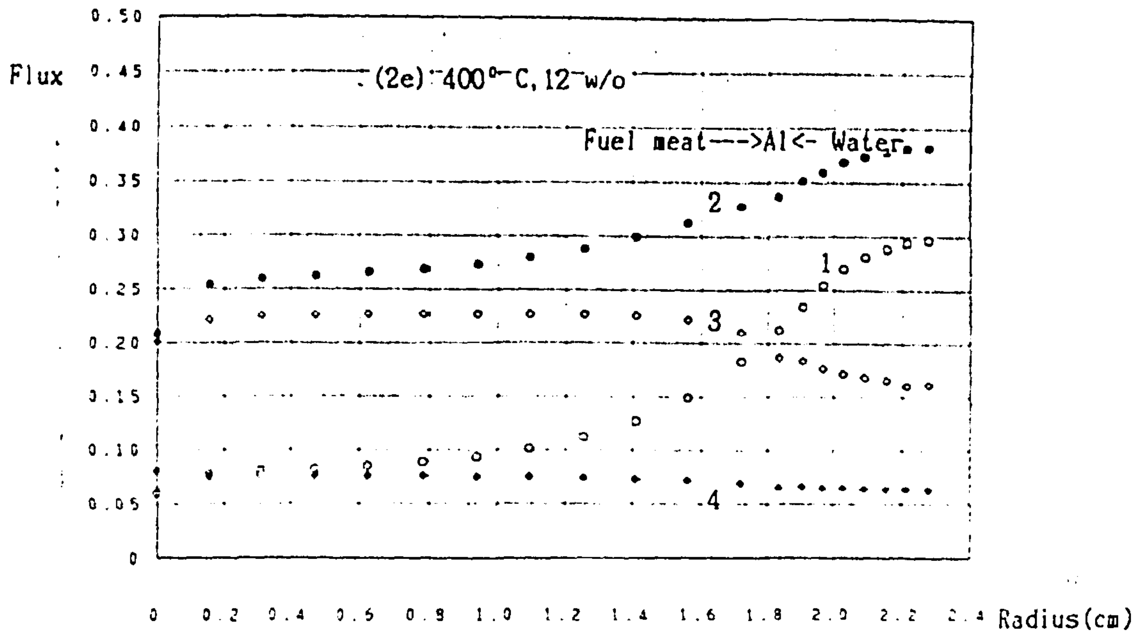

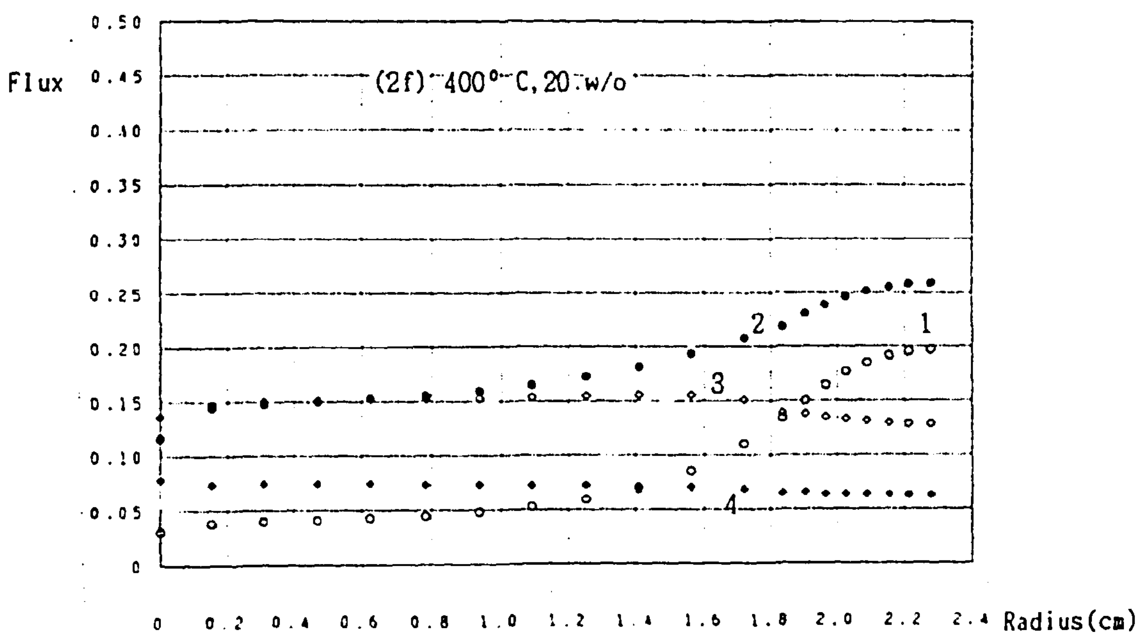

Figure 2. Thermal neutron spectrum disribution in 12 w/o and 20 w/o fuel cells at various fuel meat temperatures.Neutron groups are given by the numbers on the graphs.

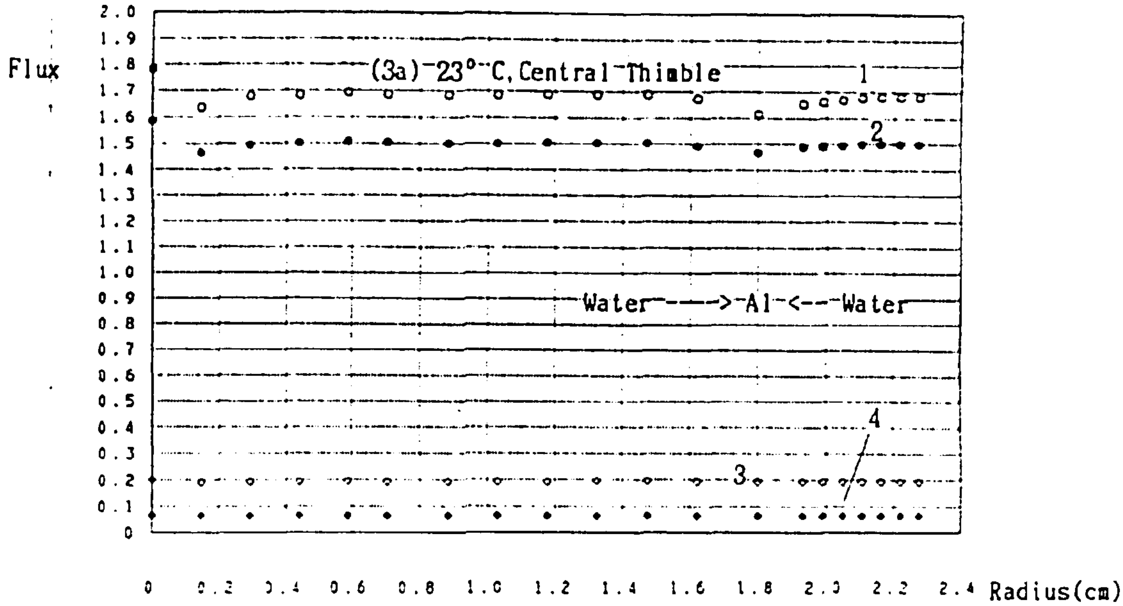

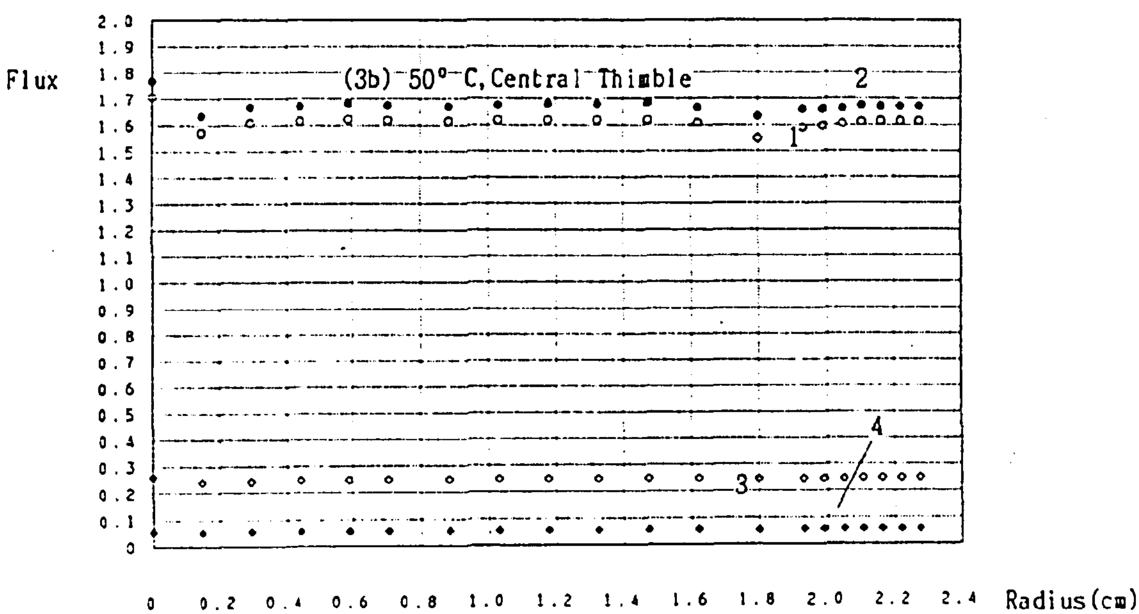

Figure 3. Thermal neutron spectrum distribution in central thimble cell at 23 ° C and 50 ° C

tron spectrum variation with temperature between the fuel and the central thimble cells is due to the difference in the moderating property of the hydrogen atoms in the fuel and water.

Conclusion

The following characteristics of TRIGA fuel can be explained and deduced from the above results:

When the fuel temperature increases, the neutron spectrum in the fuel is hardened and more neutrons escape from the fuel, thermalized and finally absorbed in the water. Furthermore, the hardening of neutron spectrum increases parasitic resonance absorption of epithermal neutrons by U-238 through the Doppler broadening effect. Both factors reduce the effective multiplication factor of the core. In addition, as the fuel and moderator are homogeneously mixed, their temperature changes simultaneously. The combination of these factors give rise to the unique large prompt negative temperature coefficient of reactivity of the TRIGA reactor. It is due to this that TRIGA reactor exhibits the so called inherent safety feature and allows the reactor to be operated in the pulsing mode.

Since the neutron spectrum of the higher uranium content fuels is harder than the 8.5 w/o fuel, their temperature coefficient of reactivity is more negative than that of 8.5 w/o fuel. Due to greater depression of the lower energy thermal neutron flux, the fission rate and temperature of TRIGA fuel do not vary linearly with its uranium content even if other factors affecting these remain unchanged.

References

1. I. Ise, Private communucations.

2. I. Otake, In evaluation of thermal neutron scattering cross sections for reactor moderators, ed. Thermalisation group in JNDC,LAERI-1181,1969.

Acknowledgement

The study was carried out with a fellowship from the Matsumae International Foundation(MIF).